Available online at www.sciencedirect.com
SCIENCE DIRECT®
Journal of Sound and Vibration 291 (2006) 1278–1287
JOURNAL OF SOUND AND VIBRATION
www.elsevier.com/locate/jsvi

Short Communication

Analytical and experimental investigation on a vibrating annular membrane attached to a central free, rigid core

Fabrizio Pinto*

InterStellar Technologies Corporation, 115 North Fifth Avenue, Monrovia, CA 91016, USA

Received 7 April 2005; received in revised form 5 July 2005; accepted 14 July 2005
Available online 2 September 2005

Abstract

The natural frequencies of a membrane-central core system are computed and compared with the experimental data from a modified capacitive microphone excited by an electrostatic actuator in a vacuum chamber under controlled temperature conditions. The observed frequencies confirm those from the theoretical model to within $\lesssim 2\%$.

1. Introduction

As pointed out in Ref. [1], a remarkable dearth of literature exists on the effects of coupling membranes to rigid objects. The author of that same reference offered a first approach to the problem of the free vibrations of an annular membrane attached to a free, rigid core in its center (historically, this question had previously been proposed as an exercise in Ref. [2]). Comparison of the theory to the data from direct experimentation in this particular case appears non-existent, although the setup discussed in Ref. [3] implicitly yields information about the asymptotic limits of a relatively very massive and very small central core.

Beyond its evident intrinsic relevance, this system also has fundamental physics and engineering interest, as it models the behavior of the membrane of a capacitive microphone loaded with a small disk permanently cemented at its center. Such a modified microphone was used in a past

*Tel.: +1 626 359 0171.
E-mail address: fabrizio.pinto@interstellartechcorp.com.

0022-460X/$ - see front matter © 2005 Elsevier Ltd. All rights reserved.
doi:10.1016/j.jsv.2005.07.027

attempt to detect the van der Waals forces between the central disk and a facing surface [4]. This effort produced initial promising results, but quantitative agreement with the predictions of quantum-electro-dynamics was only partially satisfactory. We have undertaken a comprehensive effort to greatly improve and expand on the general approach of this experiment by adopting, however, a similar force-sensing strategy. The corner-stone of correct data interpretation in an effort of this type is clearly a thorough understanding of the behavior of the membrane-disk system above. However, the authors of Ref. [4] offered a very limited discussion of the dynamics of their sensor, which may, at least in part, explain their partially unsatisfactory results.

Here, we report on the relevant facts of the theory of membrane oscillations in the presence of a central rigid core and compare our predictions to our first experimental data, obtained as part of the process of calibration of the sensor to be used in upcoming van der Waals force measurements.

2. The effect of the central core on the natural frequencies of the membrane

In this section, we review the basic theory of annular membranes with a central core [1] and expand on it to produce specific predictions of the natural frequencies of the system. The governing equation of a membrane in polar coordinates in the absence of friction and external forces can be written as

$$\nabla^2\zeta(r,\theta,t) - \frac{\sigma_M}{T_M}\frac{\partial^2\zeta(r,\theta,t)}{\partial t^2} = 0, \tag{1}$$

where $\zeta(r,\theta,t)$ is the displacement from the position of equilibrium, r,θ are the usual polar coordinates, t is the time, and T_M and σ_M are the membrane tension and surface density. Upon the usual separation of variables, the radial solution reads

$$\zeta(r) = R_{0,1}J_n\left(\frac{\omega}{v}r\right) + R_{0,2}N_n\left(\frac{\omega}{v}r\right), \tag{2}$$

where $J_n(\omega r/v)$ and $N_n(\omega r/v)$ are the Bessel and Neumann functions, respectively; $v \equiv \sqrt{T_M/\sigma_M}$; the constants $R_{0,i}$ are to be determined; and the overall solution is $\zeta(r,\theta,t) = \zeta(r)T(t)$, since we shall not consider modes with $n \neq 0$.

The boundary condition at the fixed, outer rim of the membrane requires that

$$\zeta(R_M) = R_{0,1}J_n\left(\frac{\omega}{v}R_M\right) + R_{0,2}N_n\left(\frac{\omega}{v}R_M\right) = 0. \tag{3}$$

This can be satisfied for every order n and frequency ω by choosing

$$R_{0,1} = N_n\left(\frac{\omega}{v}R_M\right), \quad R_{0,2} = -J_n\left(\frac{\omega}{v}R_M\right), \tag{4}$$

which corresponds to the solution

$$\zeta(r) = N_n\left(\frac{\omega}{v}R_M\right)J_n\left(\frac{\omega}{v}r\right) - J_n\left(\frac{\omega}{v}R_M\right)N_n\left(\frac{\omega}{v}r\right). \tag{5}$$

In order to obtain the natural frequencies of the system, let us now consider the equation of motion of the disk attached to the membrane in the hypothesis that such mass is placed exactly at

the center. In the free vibration case, the only force acting on this central flat is due to its interaction with the inner edge of the membrane and, in general, it is responsible not only for the oscillation of the center of mass of the disk, but also for possible rotations that bring it away from a plane parallel to the (x, y)-plane [1]. Here, we shall restrict ourselves to modes that cause the disk to only move parallel to the (x, y) plane, that is, the disk will only accelerate along the z-axis in the chosen reference frame with no rotation. Thus

$$F_{\text{net,flat}} = 2\pi R_{\text{flat}} T_M \left.\frac{\partial \zeta(r,\theta,t)}{\partial r}\right|_{r=R_{\text{flat}}} = M_{\text{flat}} \frac{\mathrm{d}^2 z_{\text{flat}}}{\mathrm{d}t^2}, \tag{6}$$

where M_{flat} and R_{flat} are the mass and the radius of the flat disk, respectively. Since the outer edge of the disk coincides with the inner radius of the annular membrane, we have the additional geometric constraint that $z_{\text{flat}} = \zeta(R_{\text{flat}}, \theta, t) = \zeta_C(t)$ (Fig. 2) and thus $\ddot{z}_{\text{flat}} = \ddot{\zeta}(R_{\text{flat}}, \theta, t)$, or

$$2\pi R_{\text{flat}} T_M \frac{\partial \zeta(r,\theta,t)}{\partial r} = M_{\text{flat}} \left.\frac{\mathrm{d}^2 \zeta(r,\theta,t)}{\mathrm{d}t^2}\right|_{r=R_{\text{flat}}}. \tag{7}$$

By assuming the harmonic dependence $T(t) = T_{0,1}\cos\omega t + T_{0,2}\sin\omega t$ for the time part of the solution,

$$\left.2\pi R_{\text{flat}} T_M \frac{\partial \zeta(r,\theta,t)}{\partial r}\right|_{r=R_{\text{flat}}} = -\omega^2 M_{\text{flat}} \zeta(R_{\text{flat}}, \theta, t). \tag{8}$$

By making use of the recurrence relation $J_{n+1} = (n/x)J_n - J_n'(x)$ (and similarly for the Neumann functions) [5] to rewrite the above equation in terms of the solution at Eq. (5), we finally obtain, if $n = 0$

$$\begin{aligned}&\omega^2 M_{\text{flat}}\left[N_0\left(\frac{\omega}{v}R_M\right)J_0\left(\frac{\omega}{v}R_{\text{flat}}\right) - N_0\left(\frac{\omega}{v}R_{\text{flat}}\right)J_0\left(\frac{\omega}{v}R_M\right)\right]\\ &\quad = 2\pi R_{\text{flat}} T_M \frac{\omega}{v}\left[N_0\left(\frac{\omega}{v}R_M\right)J_1\left(\frac{\omega}{v}R_{\text{flat}}\right) - J_0\left(\frac{\omega}{v}R_M\right)N_1\left(\frac{\omega}{v}R_{\text{flat}}\right)\right].\end{aligned} \tag{9}$$

From Eq. (8), we can see that, if the mass of the central disk becomes relatively large, the inner boundary is approximately fixed just as the outer one, which corresponds to the typical problem of an annular membrane clamped at both boundaries. We can see above that, if $\omega^2 M_{\text{flat}} \gg 2\pi R_{\text{flat}} T_M \omega/v$, or $\sigma_{\text{flat}} \gg 2T_M/\omega R_{\text{flat}} v = 2\sqrt{T_M \sigma_M}/\omega R_{\text{flat}}$, where σ_{flat} is the surface density of the central disk ($M_{\text{flat}} = \pi R_{\text{flat}}^2 \sigma_{\text{flat}}$), the term at right-hand side can be neglected and we obtain, in this limit of a very massive central core

$$N_0\left(\frac{\omega}{v}R_M\right)J_0\left(\frac{\omega}{v}R_{\text{flat}}\right) - N_0\left(\frac{\omega}{v}R_{\text{flat}}\right)J_0\left(\frac{\omega}{v}R_M\right) = 0. \tag{10}$$

This indeed is the known equation for the modes of oscillation of an annular membrane fixed at both its inner and outer radii [1,6].

Let us now rearrange Eq. (9) as

$$N_0\left(\frac{\omega}{v}R_M\right)J_0\left(\frac{\omega}{v}R_{\text{flat}}\right)\left[1-\frac{2\sqrt{T_M\sigma_M}}{\sigma_{\text{flat}}R_{\text{flat}}\omega}\frac{J_1\left(\frac{\omega}{v}R_{\text{flat}}\right)}{J_0\left(\frac{\omega}{v}R_{\text{flat}}\right)}\right]$$
$$-J_0\left(\frac{\omega}{v}R_M\right)N_0\left(\frac{\omega}{v}R_{\text{flat}}\right)\left[1-\frac{2\sqrt{T_M\sigma_M}}{\sigma_{\text{flat}}R_{\text{flat}}\omega}\frac{N_1\left(\frac{\omega}{v}R_{\text{flat}}\right)}{N_0\left(\frac{\omega}{v}R_{\text{flat}}\right)}\right]=0, \tag{11}$$

which shall be used below to interpret our experimental data.

3. Experimental investigation

3.1. Measurement setup

The experiment was carried out by means of a "half-inch" (nominal) condenser microphone, model 7013 made by ACO PACIFIC, Inc. [7] (equivalent to Bruel and Kjaer Type 4134/4192) coupled to a PS9200-2 channel power supply and a 4012 Preamplifier made by the same company. The response of the microphone was studied by an electrostatic actuator approach similar to that typical of capacitive microphones in air (see, for instance, Ref. [8, Chapter 15]). In our case, the grounded microphone membrane is stimulated by applying a known potential at the desired signal frequency between it and a $\frac{1}{4}\lambda$ flat surface, 1 in (2.54 cm) diameter metallic mirror. The mirror substratum is 6061-T6 aluminum coated by a conducting, first surface layer of gold with a rms surface roughness $<175\,\text{Å}$.

Initially, the device was placed inside a vacuum chamber located on a vibration-dampening table at ambient pressure. Inside the chamber, several manual translational and rotational micrometers were used to establish the appropriate distance range between the microphone membrane and the gold mirror (Fig. 1). The appropriate zero of this motion is determined by establishing the contact point between the microphone membrane and the electrostatic actuator where the output signal from the microphone breaks down. Additional, nanometer-level positioning of the electrostatic actuator is available at all times via a piezoelectric nano-positioner with a maximum range of motion of 65 μm. Once the appropriate position settings are achieved and after routing all electrical connections through a feedthrough plate, the vacuum chamber is sealed and pumping is initiated until the pressure drops below $P_{\text{chamber}}<10^{-4}$ Torr. The response of the microphone changes drastically as the pressure drops from ambient to its final value. As expected, an overall decrease in background noise and the appearance of a marked resonant behavior of the membrane are observed. In order to achieve additional environmental control, the temperature of the vacuum chamber was automatically maintained at $(30.0\pm0.5)\,^{\circ}\text{C}$ via electrical heaters.

As a first step, we explored the response of the free (no central core) membrane to a signal containing both a DC and an AC component (the large DC component suppresses the microphone response at twice the forcing frequency [8]). With reference to Fig. 2, typical values used were: $H_0=0.5\times10^{-3}$ m; $V_0=25$ V; $V_{0p}=1$ V (see also Table 1).

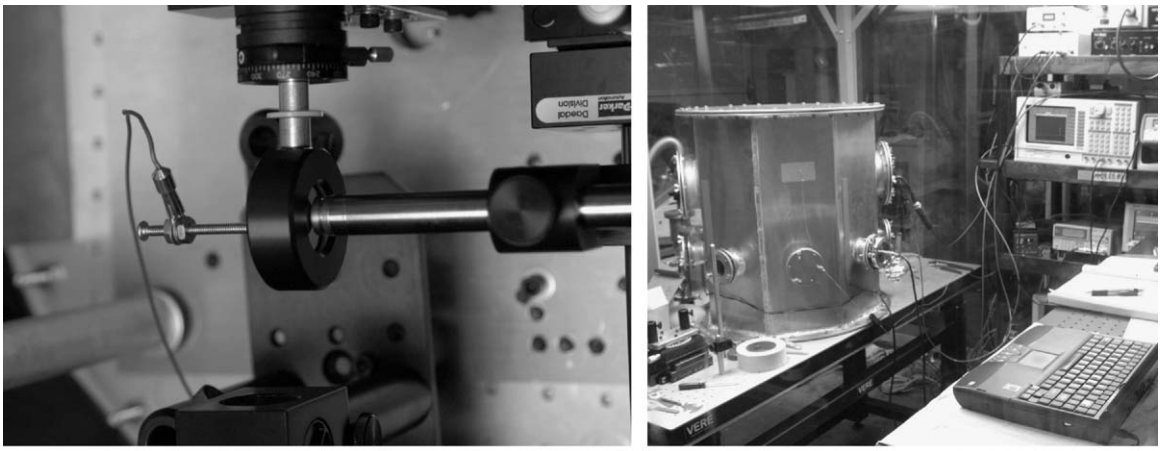

(a) (b)

Fig. 1. (a) Sensor inside the vacuum chamber and (b) equipment used for the experiment.

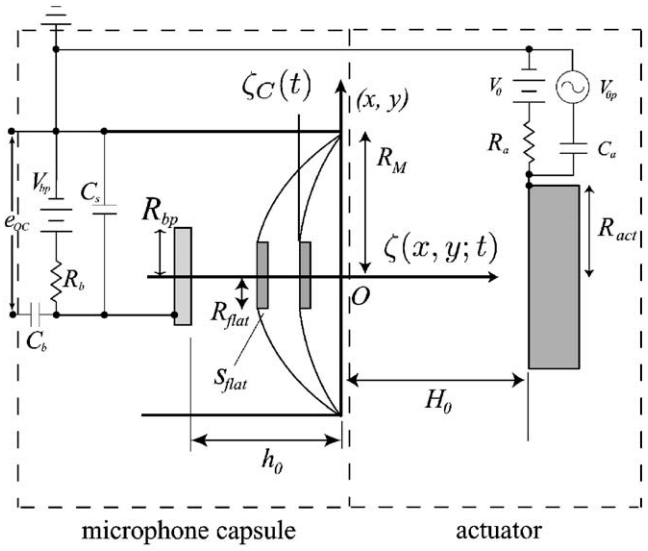

Fig. 2. Schematic diagram of the capacitive sensor and electromagnetic actuator.

A rough estimate of the membrane resonance frequency ($\approx 21\,\text{kHz}$) was obtained by using an FFT analyzer and a signal generator in sweep mode.

The dynamics of a microphone membrane undergoing forced oscillations due to a pressure of the electrostatic type is extremely well understood [9,10]. What is important here is that the system is expected to resonate sharply near its natural frequencies and that the response of the system near resonance is adequately described by a Lorentz best-fit [11]. In our case, the resonance frequency was found at $(21,164.67 \pm 0.02)\,\text{Hz}$ with a quality factor $Q \simeq 526$ or, equivalently, a

Table 1
Properties of the capacitive sensor

Property	Symbol	Units	Nominal	Computed	Observed
Microphone capsule					
Outer radius	R_{mic}		0.635		
Free membrane					
Radius	R_M	cm			$0.495(= 78\% R_{\mathrm{mic}})$
Thickness	s_M	μm	3.0		
Volume density	ρ_M	$\mathrm{g/cm^3}$	8.027		
Surface density	σ_M	$\mathrm{g/cm^2}$	—	2.408×10^{-3}	
Fundamental	$\nu_{M,0}$	Hz	—	—	21,164.67; $Q_{M,0} = 526$
Tension	T_M	dyne/cm	—	1.804×10^6	
Central core					
Radius	R_{flat}	cm	0.125		0.131
Thickness	S_{flat}	cm	0.050		
Volume density	ρ_{flat}	$\mathrm{g/cm^3}$	2.201		
Surface density	σ_{flat}	$\mathrm{g/cm^2}$	0.11		
Electrostatic actuator					
Radius	R_{act}	cm	2.54		
Distance to membrane	H_0	cm			0.05
Membrane and core					
Fundamental	ν_0	Hz		6064.5	6064.55 ± 0.02; $Q_0 = 497$
First natural frequency	ν_1	Hz		37,378.3	$38{,}102.83 \pm 0.07$; $Q_1 = 415$
Second natural frequency	ν_2	Hz		75,004.8	$74{,}851.0 \pm 0.5$; $Q_2 = 348$

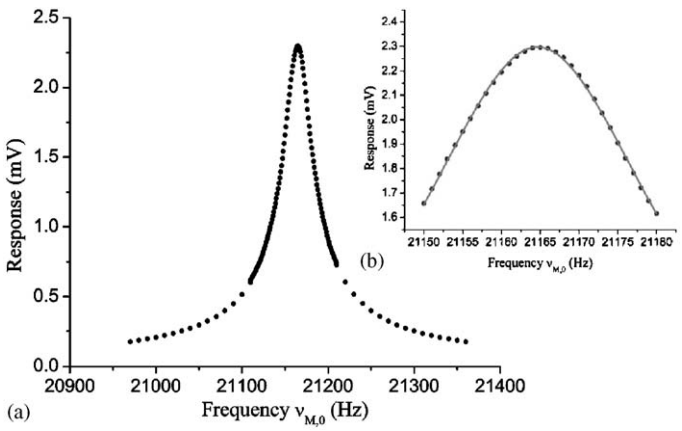

Fig. 3. Free membrane response: (a) large scale and (b) detail.

relaxation time $\tau \simeq 0.156\,\mathrm{s}$; in Fig. 3 are displayed the data within a wide range of the resonance and, in the right inset, the data in its immediate vicinity and used for the Lorentz fit. The slight shift to lower frequencies due to dampening in this case is $\sim 10^{-2}$ Hz and shall be neglected in what follows.

The fundamental frequency of the complete circular membrane constrained at its outer edge is given by [8–11]

$$f_1 = \frac{2.4048}{2\pi R_M}\sqrt{\frac{T_M}{\sigma_M}}. \tag{12}$$

With the values given for R_M and the volume density ρ_M of the 303 stainless steel used to manufacture the membrane, it is immediate to obtain estimates of both its surface density and tension (Table 1).

The next step was to install the flat disk onto the center of the membrane which acts as a free core. In our case this is a 2.5 mm diameter disk of fused silica (Corning 7980 of UV Grade), 0.50 ± 0.05 mm thick, optically polished on the side facing the electrostatic actuator at 40/20 scratch/dig, <7 Å, flat to $\lambda/4$ (Table 1 and Ref. [12]). The side permanently cemented to the steel membrane of the capacitative sensor is ground to a finish. The process of installation was carried out by means of a vacuum compatible, hardener/adhesive compound rated for pressures as low as 10^{-8} Torr. A mask was prepared by enlarging an already existing hole in the protective grid of the microphone so that the small flat could be slipped through it. The procedure was monitored via a microscope/CCD system for any further adjustments (Fig. 4).

From the practical standpoint, cementing the disk to the membrane presented us with the following options: (1) to deposit only an extremely small amount of epoxy so that just the central part of the flat disk would be effectively attached to the membrane; (2) to deposit more than necessary and obtain some excess leakage to the sides. The former option would have resulted in a "cleaner" finished product, but with the resulting difficulty in characterizing the boundary conditions under the disk itself. The latter option, which we chose, as shown in Fig. 4 (*right*), resulted in an epoxied area larger than that of the flat itself because of the leaked excess, but it yielded a sure bond to the membrane everywhere around the circumference of the disk. Digital imaging of the finished process after the epoxy was cured allowed us to assess the effective values

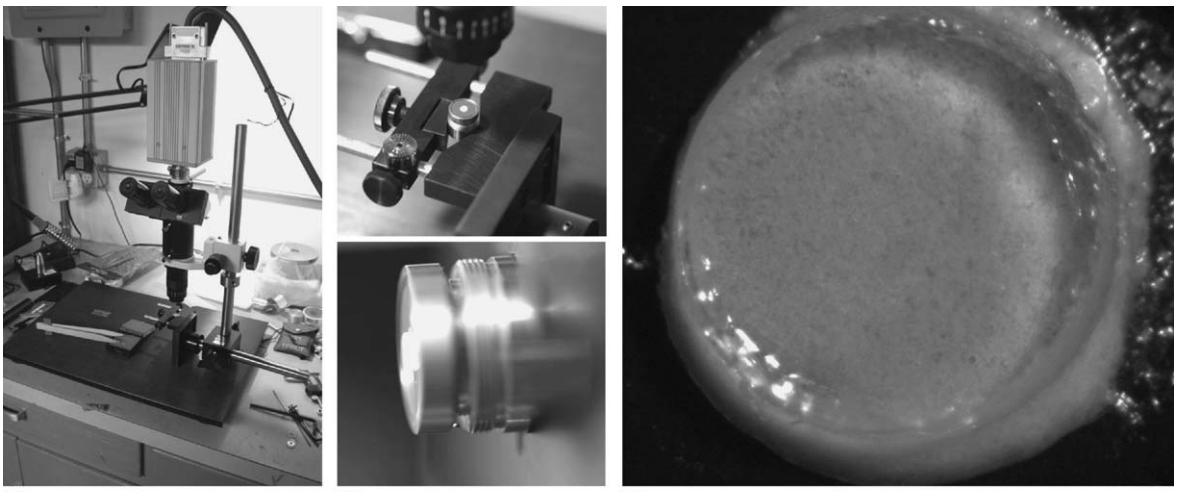

Fig. 4. (a) CCD system; (b) microphone capsule and (c) cemented flat disk.

to be used in our model. We also verified that the core was cemented off-center by $\approx 2 \times 10^{-2}$ cm, or within 2% of the diameter of the membrane (Table 1).

3.2. Experimental data

The same procedure as in the case of the free membrane was carried out once the membrane and disk system had been reassembled in the vacuum chamber as previously described. By proceeding with a thorough scan of the response of the system in both sweeping and manual modes in the 0–100 kHz region, the three following resonances were identified and characterized, and their position determined from a nonlinear Lorentz-fit conducted by means of the ORIGIN data analysis package [13]: $\nu_{0,\mathrm{obs}} = (6064.55 \pm 0.02)$ Hz (Fig. 5, *left* and *top middle inset*), $\nu_{1,\mathrm{obs}} = (38{,}102.83 \pm 0.07)$ Hz (*top right inset*), and $\nu_{2,\mathrm{obs}} = (74{,}851.0 \pm 0.5)$ Hz (*bottom right inset*), respectively. The experimental errors on the frequencies thus obtained only reflects the best estimate of the instrumental error and of that resulting from the Lorentz-fitting procedure under conditions of ideal repeatability. In reality, the resonance frequencies are observed to fluctuate by $\lesssim 10^2$ Hz, or $\lesssim 2\%$ of their average value over a period of hours, most likely due to the effect upon the membrane tension of the temperature fluctuations of the apparatus. Under these conditions, better estimates are obtained by gathering fewer resonance data within a relatively short time dictated by experience (usually $\lesssim 15$ min). For an example of the decreased quality in the case of a larger data set acquired over a longer period of time, see the first natural frequency resonance (Fig. 5, *top right inset*).

The magnitude of the response signal is not going to be addressed in the present model and will be considered in detail elsewhere. However, it is appropriate to remark here that the average

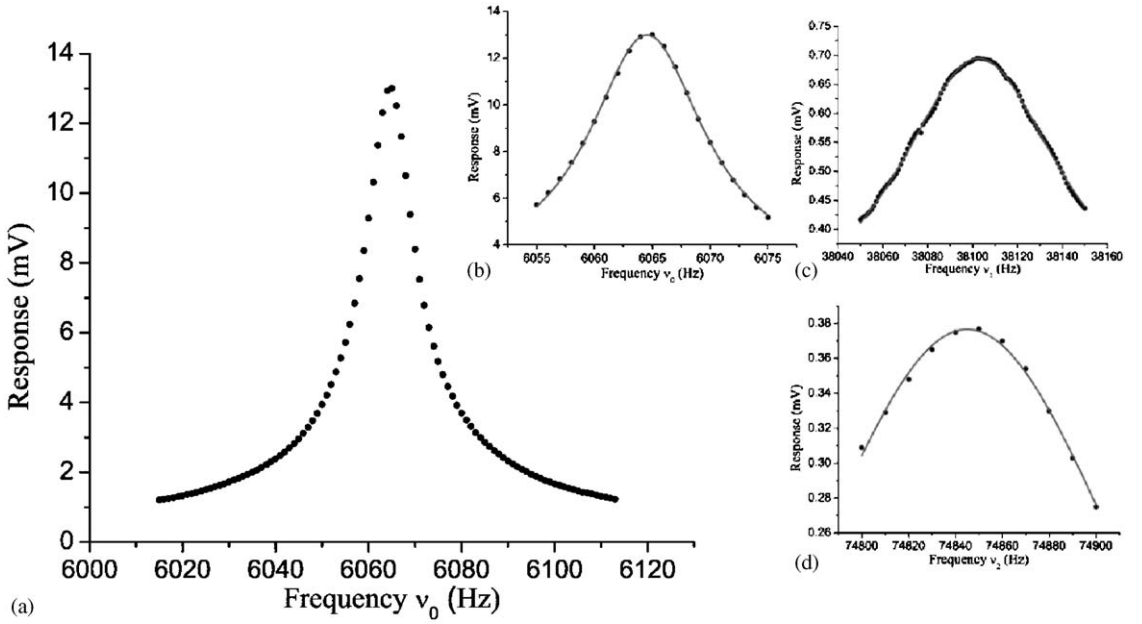

Fig. 5. (a) Flat/membrane fundamental frequency and (b)–(d) first two natural frequencies.

displacement of the membrane over its area at any time is smaller at higher frequencies because of the oscillating radial nature of the solution at Eq. (5). Therefore, the output signal is observed to become smaller for higher natural frequencies. This qualitatively explains the much higher fundamental resonance peak ($\approx 10\,\mathrm{mV}$) compared to that at the first natural frequency ($\approx 1\,\mathrm{mV}$). In the case of the second natural frequency, it was actually necessary to polarize the electrostatic actuator to a voltage $V_0 = 250\,\mathrm{V}$ (as opposed to the value $V_0 = 25\,\mathrm{V}$ typically used) with an AC signal $V_{0p} = 5\,\mathrm{V}$ (as opposed to a typical $V_{0p} = 1\,\mathrm{V}$) in order to obtain relatively noise-free data. By normalizing the observed second natural frequency resonance peak by a total factor of 50, we find a response $\approx 8\,\mu\mathrm{V}$. An additional factor that, in practice, contributes to relatively smaller signals at higher resonant frequencies is the decrease in the quality factor Q and the corresponding increase in the dampening of the membrane. This reflects the general rule that higher modes damp out more rapidly than lower modes and that the dampening losses increase as the membrane becomes more segmented [11].

4. Discussion and conclusions

In order to use the membrane-central core model to analyze our experimental data, a Mathematica notebook [14] was coded to explore the behavior of Eq. (11) for realistic values of our physical parameters. If the quantities T_M, σ_M, R_{flat}, σ_{flat}, and R_M are assigned, the solutions can be given in graphical terms, as shown in Fig. 6, where the left-hand side of Eq. (11) is shown as a function of $\omega = 2\pi\nu$.

Substitution of the nominal parameters in Table 1 known from manufacturers' specifications and from our observations of the free membrane yields the following predicted resonant frequencies: $\nu_{0,\mathrm{comp}} = 6071.9\,\mathrm{Hz}$, $\nu_{1,\mathrm{comp}} = 36{,}732.6\,\mathrm{Hz}$, and $\nu_{2,\mathrm{comp}} = 73{,}758.9\,\mathrm{Hz}$. These values are within $\lesssim 4\%$ of the observed values for the higher natural frequencies and within $\sim 0.1\%$ for the fundamental frequency. Agreement with observation improves remarkably by choosing the observed value of the flat disk diameter and a thickness approximately 5% less than the nominal value, corresponding to $\sigma_{\mathrm{flat}} = 0.104\,\mathrm{g/cm^3}$ (this is only half of the manufacturer's own thickness tolerance). In this case, we predict: $\nu_{0,\mathrm{comp}} = 6{,}064.5\,\mathrm{Hz}$, $\nu_{1,\mathrm{comp}} = 37{,}378.3\,\mathrm{Hz}$, and $\nu_{2,\mathrm{comp}} = 75{,}004.8\,\mathrm{Hz}$. In the case of $\nu_{0,\mathrm{comp}}$ and $\nu_{2,\mathrm{comp}}$, these values are to within less than 0.2% of the observed values.

These minor parameter adjustments are certainly consistent with the uncertainties introduced by the bonding process, the remaining temperature-related fluctuations, and additional errors due

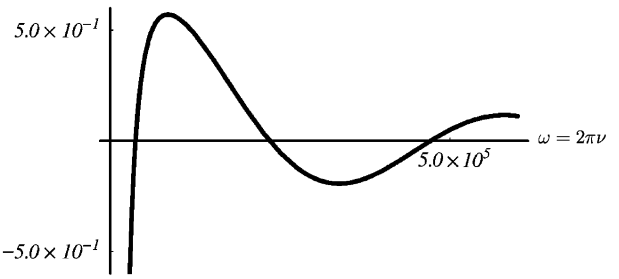

Fig. 6. Showing the left-hand side of Eq. (11) and its zeroes.

to such quantities as the nominal volume densities of both stainless steel and fused silica. The frequency data of the membrane-flat disk system conform very closely to the expected values computed from our model and they confirm the validity of Eq. (11).

Acknowledgments

Thanks are due to Gerry Verwick of VERE, Inc. for producing the very specific vacuum chamber and other custom supporting equipment used in this project and to Noland Lewis of Aco Pacific, Inc. for in-depth conversations and correspondence on the characteristics of the microphone used in the experiment described herein.

References

[1] C.Y. Wang, Vibration of an annular membrane attached to a free, rigid core, *Journal of Sound and Vibration* 260 (2003) 776–782.
[2] K.F. Graff, *Wave Motion in Solids*, Dover, New York, 1975, p. 271 (Prob. 4.7).
[3] P.A.A. Laura, S. La Malfa, S.A. Vera, D.A. Vega, M.D. Sánchez, Analytical and experimental investigation on vibrating membranes with a central point support, *Journal of Sound and Vibration* 221 (1999) 917–922.
[4] S. Hunklinger, H. Geisselman, W. Arnold, A dynamic method for measuring the van der Waals forces between macroscopic bodies, *Review of Scientific Instruments* 43 (1972) 584–587.
[5] G. Arfken, *Mathematical Methods for Physicists*, Academic, Orlando, 1985.
[6] F.F. Cap, *Mathematical Methods in Physics and Engineering with Mathematica*, Chapman & Hall/CRC, Boca Raton, 2003, p. 265.
[7] See specifications as http://www.acopacific.com/chart.html
[8] G.S.K. Wong, T.F.W. Embleton (Eds.), *AIP Handbook of Condenser Microphones*, American Institute of Physics, New York, 1995.
[9] I.B. Crandall, *Theory of Vibrating Systems and Sound*, Van Nostrand, New York, 1927.
[10] P.M. Morse, K.U. Ingard, *Theoretical Acoustics*, Princeton University Press, Princeton, NJ, 1986.
[11] L.E. Kinsler, A.R. Frey, A.B. Coppens, J.V. Sanders, *Fundamentals of Acoustics*, Wiley, New York, 2000, p. 97.
[12] See http://www.valleydesign.com/7940.htm
[13] http://www.originlab.com/index.aspx?s=8#origin
[14] S. Wolfram, *The Mathematica Book*, *fourth ed.*, Cambridge University Press, Cambridge, 1999.